

See discussions, stats, and author profiles for this publication at: <https://www.researchgate.net/publication/302933905>

# Innovative Solar Array Drive Assembly for CubeSat Satellite

Conference Paper · May 2016

CITATIONS

0

READS

1,504

4 authors, including:



**Michele Marino**

IMT srl

8 PUBLICATIONS 57 CITATIONS

[SEE PROFILE](#)



**Andrea Negri**

10 PUBLICATIONS 45 CITATIONS

[SEE PROFILE](#)



**Massimo Perelli**

IMT, Ingegneria Marketing Tecnologia, Italy, Roma

14 PUBLICATIONS 53 CITATIONS

[SEE PROFILE](#)

# INNOVATIVE SOLAR ARRAY DRIVE ASSEMBLY for CUBESAT SATELLITE

**Michele Marino<sup>(1)</sup>, Andrea Negri<sup>(2)</sup>, Massimo Perelli<sup>(3)</sup>, Raffaele Palamides<sup>(4)</sup>**

<sup>(1)</sup> *IMT srl, Via Carlo Bartolomeo Piazza 30, +390644292634, [michele.marino@imtsrl.it](mailto:michele.marino@imtsrl.it)*

<sup>(2)</sup> *IMT srl, Via Carlo Bartolomeo Piazza 30, +39064429263, [andrea.negri@imtsrl.it](mailto:andrea.negri@imtsrl.it)*

<sup>(3)</sup> *IMT srl, Via Carlo Bartolomeo Piazza 30, +390644292634, [massimo.perelli@imtsrl.it](mailto:massimo.perelli@imtsrl.it)*

<sup>(4)</sup> *IMT srl, Via Carlo Bartolomeo Piazza 30, +390644292634, [raffaele.palamides@imtsrl.it](mailto:raffaele.palamides@imtsrl.it)*

## ABSTRACT

The CubeSat satellite is a smart option for reliable and low cost space mission development. Growing CubeSat performances lead to more extensive nanosatellite application. Currently, Telecommunication and Earth Observation missions are under development both in single and constellation configurations. The main targets for the future nanosatellite are: accurate attitude pointing, high data rate transfer, increased power generation. The on board power/energy availability reduces or limits the CubeSat performances in terms of processing capabilities, power transmission and attitude/orbit maneuvers. Following these constraints, the IMT has developed an innovative unit, named nano-Solar Array Drive Assembly (SADA) for 3U CubeSat, with the aim of increasing the photovoltaic energy generation (up to an average 35W EOL). It is composed by two independent Solar Arrays (Wings Assembly) and Rotatory Mechanisms / Logical Unit (SAC – Solar Array Control). The aim of SADA is to align constantly the two Solar Arrays to the Sun direction, around one axis. The rotatory system is composed by drive gear sets, stepper motors and slip rings. The high value of gearhead reduction ratio and two dedicated photodiodes (as solar sensors) allow a fine pointing accuracy ( $<5^\circ$ ). Several operation modes are implemented and controlled by the On Board Computer through the I<sup>2</sup>C and CAN buses: autonomous (sun detection and pointing), slave or cooperative. An advanced and smart control algorithm was developed and implemented in the logic unit. The Solar Array points along the maximum solar flux direction, maximum output speed up to  $4^\circ/\text{s}$  (step size  $0.004^\circ$ ). A system failure control avoids the thermal and power damaging in case one or both wings are blocked. SADA is fully compliant with all CubeSat form factor (3U or greater) and BUS (CSKB – CubeSat Kit Bus). The Solar Wings, during the launch phase, are stowed beside the CubeSat structure (opposite side faces). The overall thickness is less than 9 mm, compliant to ISIPOD dispenser. The Logical and Drive unit (SAC), small (90 x 90 x 12 mm) and light (185 gr), is allocated

inside the satellite. The Wings are electrically connected to the SAC, by means of two 16 channels slip rings (1A per contact) for a continuous rotation, without cable saturation. The Alignment Calibration System assures that the unit runs correctly up to 10 mm of misalignment between the SAC and the geometric satellite center, along Z direction. The generated power is not handled by SAC, but by PDU through Standard Molex Connectors. The two wings, stowed during the launch phase, are deployed in orbit. In order to increase the system reliability, the deployment is based on two redundant thermal cutter systems. In the final configuration, the 3U CubeSat has two wings, each one 300 x 300 mm and 36 AzurSpace 3J solar cells. The release and rotatory mechanisms of the two wings are independent, it means that a failure occurred in one wing will not affect the other one. The SADA project is supported by Italian Public Co-Funds (POR FESR 2007/2013 Lazio Region [1]) and the TRL level is 4/5. Mechanical and electrical functional tests are done in the relevant environment. The system is tested in the relevant environment condition to assure the right pointing accuracy and pointing algorithm functions. To increase the reliability in radiation environments, COTS components have been selected depending on radiation behavior to reach 20 Krads (TID) as minimum. The paper describes the mechanical / electrical SADA architecture and the reached test results. Furthermore, critical elements and the relevant solutions will be presented.

## 1. INTRODUCTION

Thanks to the technology improvements is possible to realize small subsystems or small units with the same performances w.r.t. the big one of few years ago. The miniaturization contributes to increment the number of micro and nanosatellite missions. Small satellites have become more attractive due to lower development costs and shorter lead times. Nowadays is possible to use CubeSat (3U or 6U) for Earth Observation and Telecommunication missions. Even if the MEMS allows to reduce volume and mass, the available surface for solar array is limited on CubeSat satellite. Several deployment systems are used in the space, some of these are orientable. The IMT has designed an Orientable Solar Array compatible to 3U CubeSat standard. Solar Array Drive Assembly (SADA) with its power transfer assembly is an important unit for high performance missions of 3-axis stabilized satellite. The main functions are:

- Rotating solar panels and making normal of solar arrays surface to coincide with solar light beam in order to obtain the maximum energy. For sun-synchronous orbit, 1 degree of freedom is used for driving solar array to track solar light beam;
- Transferring power and signals (solar array status parameters, sun-sensor information) to the satellite bus even during the rotations;

- SADA performs several operation modes, such as: tracking mode, sun acquisition mode, hold mode, pointing mode, other custom modes.

SADA is designed for a large range of applications where is required high power consumption, as Earth Observation, Telecommunications (High Data Rates Transmissions) and Scientific.

The main goal of SADA is to generate 40Wh solar power energy (BOL) in 3U Cubesat. A NASA study (State of Art [2]) roughs out the trend of the average orbit power (Figure 1). The red dot highlights the performances of SADA respect to the other systems.

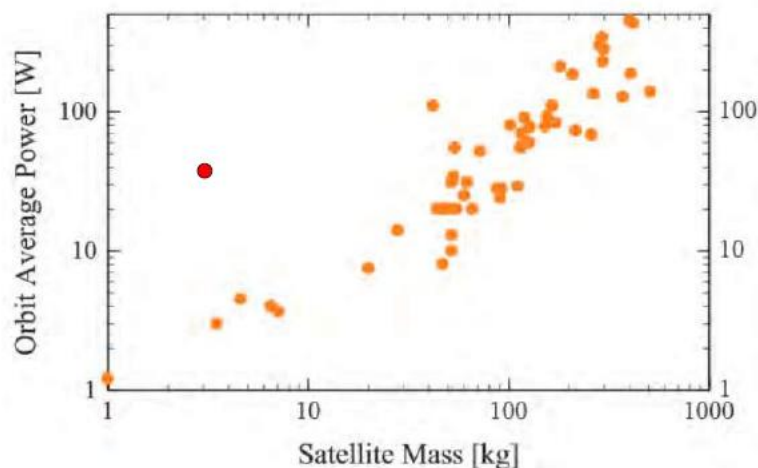


Figure 1: Orbit Average Power in function of Satellite Mass. Red dot report a 3U Cubesat with SADA

## 2. GENERAL ARCHITECTURE

SADA is composed by the Solar Array Control Unit (SAC) and two Solar Array Drive Mechanisms (SADM). The Wings are mounted symmetrically along the Z body satellite plane (Figure 2), the SAC is located inside the satellite near the COG (Center of Geometry). The dimensions are compliant to CubeSat standard (Thickness internal unit < 120 mm, stowed solar array < 8 mm).

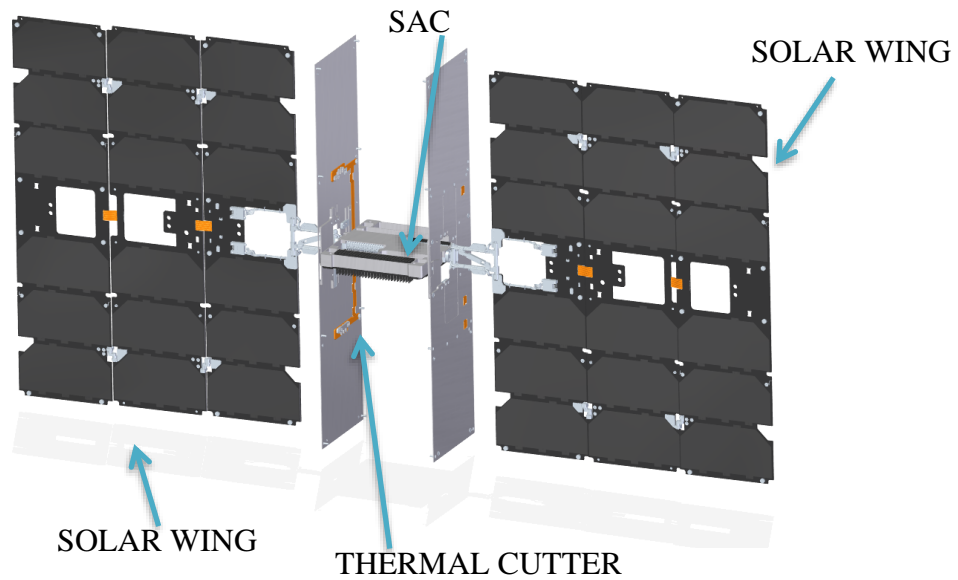


Figure 2: SADA General Architecture

The SAC has double functions:

- Drive the Solar Array Wings;
- Energy Power Transfer to EPS Subsystem.

The Solar Array Panels can be rotated independently in both forward or reverse directions, as well as transfer power, signal and grounding from the Solar Array to the satellite. The SADA has a precise rotational resolution ( $0.004^\circ$ ) and sun pointing accuracy ( $< 5^\circ$ ); it has a maximum operational speed of  $4^\circ/\text{s}$ .

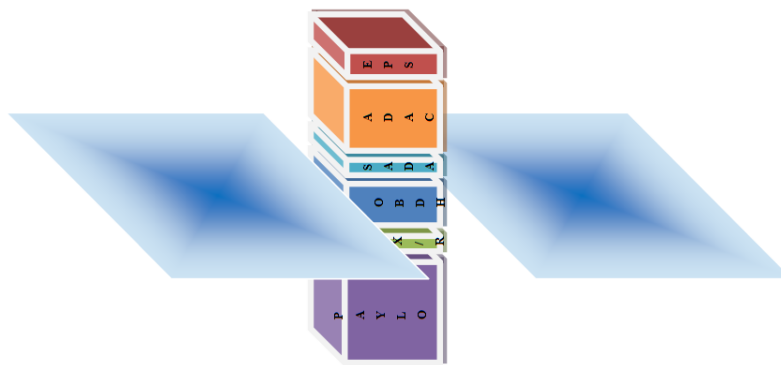


Figure 3: SADA in the 3U Cubesat

To obtain these performances, two micro stepper motors are used in the SAC. The motors, able to run in space conditions (HVAC lubricate), have a micro-gearheads (1:4096) with high rotation resolution ( $> 0.004^\circ$ ). The motors are driven by means of two independent circuits, to increase the reliability of system, handled by a microcontroller.

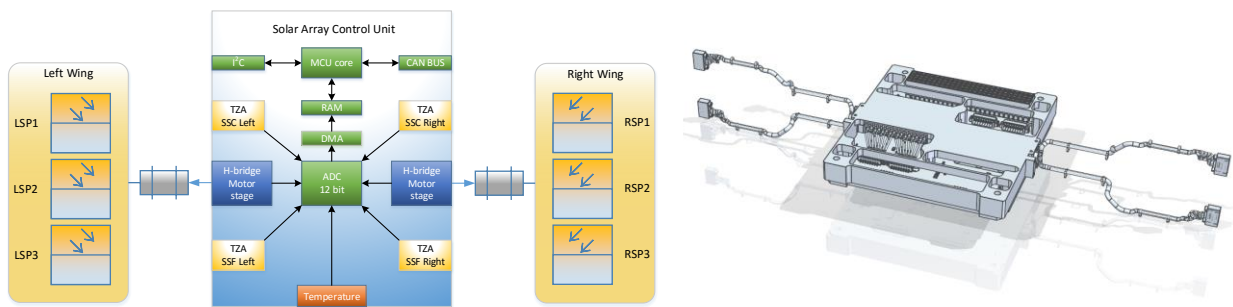


Figure 4: The SAC. Left: SAC Architecture. Right: CAD view

Two thermal cutter release mechanisms, located on the structure walls, allows the solar arrays to deploy at command received. Each thermal cutter system is composed by two cutter points, connected together thanks a flex PCB. After the release, two independent solar arrays are deployed. Each solar array is composed by three panels and N°18 3J solar cells. Up to 36 Triple Junction solar cells can be mounted on the SADA to obtain  $0.1\text{m}^2$  active area (40 Wh average power). A panel is joint to the others through a flat cable, 6S3P or 3S6P configurations can be used depending on Satellite Bus. The yoke mechanism assures the right movements and mechanical connection to the Satellite structure. The Yoke has a compensating system to reduce the internal subsystem allocation problems; the SAC can be shifted from the satellite geometry center up to 10 mm along the Z direction without restriction to the wing rotation. In addition, the yoke gives the structural support to the 16 wires cable, used for signals and power. Two photodiodes (fine and coarse) and temperature sensor, enable the SADA to run in autonomous mode, detects the sun and tracks it.

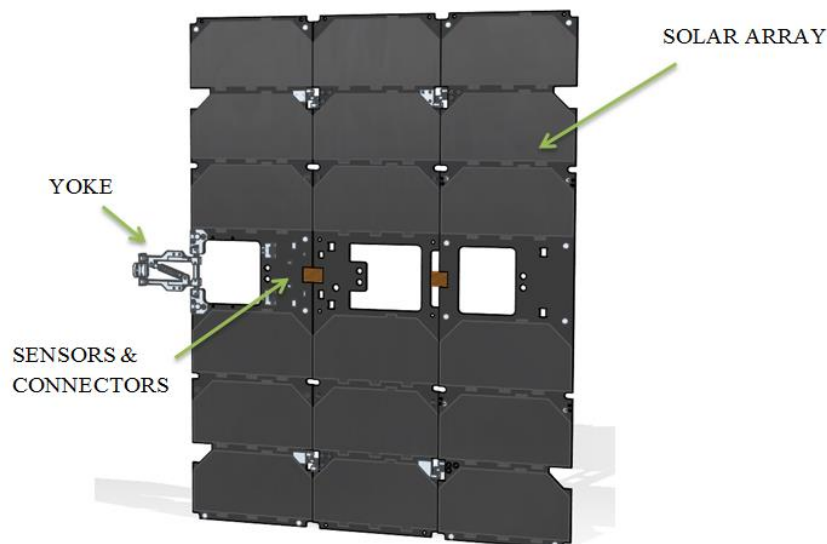


Figure 5: Yoke and SOLAR WING

### 3. ELECTRONICS DESIGN

This section describes the SADA electronics design. Figure 4 shows the SADA block diagram for the solar panel deployment and sun tracking control. Each SADA wing is composed by three solar panels and it is stowed in a thickness lower than 9mm. Two stepper motors, powered by lower voltage, drive the mechanism for the sun tracking. A gearhead on each motor allows the motor torque improvement. The Solar Array Control board (SAC) is equipped with a microcontroller beside other control logic (i.e. sensors) and power modules for the motor energy handling.

#### 3.1. Solar panels

One wing is composed by three solar panels with six 3G30A AzurSpace solar cells on each panel. Figure 6 shows the SADA wing with solar panels in a 3S/2P configuration. The SADA can be configured both 3S6P and 6S3P configurations, depending on satellite BUS voltage.

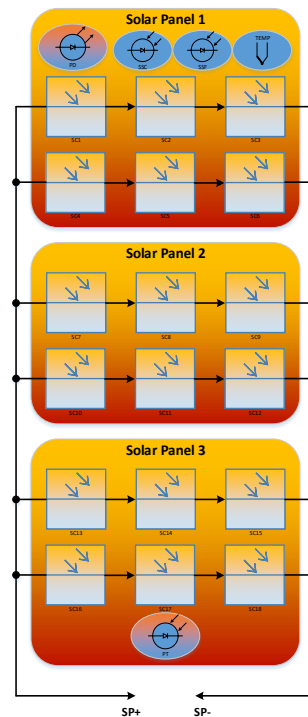


Figure 6 – SADA wing configuration

The AzurSpace solar cell has an output voltage of 2.35V and a current of 0.5A. In 3S/2P configuration each wing yields 7V@3A between SP+ and SP- terminal. When the wings are in the maximum solar tracking point, the available power is about 42W. One photodiode and one phototransistor are used to get feedback about stowed or deployed configurations:

- when they are face to face, the photodiode emits light pulses that are received by phototransistor – (stowed configuration);

- when the wings are deployed, no light pulses are received by phototransistor.

Two photodiodes (SSC – Sun Sensor Coarse and SSF – Sun Sensor Fine) are used for maximum power point tracking and finally a temperature sensor is used to monitor the panel heating under sun light beam. Figure 7 shows the solar cells string configuration. The blocking diodes avoid losing string when one cell is shadowed or broken.

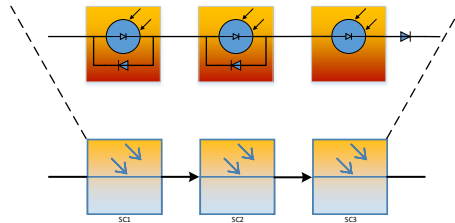


Figure 7 – Solar cell string configuration

Once in orbit, if the deployment goes wrong, at least one panel (3S/2P) having facing out can provide power to the EPS subsystem.

### 3.2. Thermal cutter actuators

In stowed configuration the solar panels are blocked using a Dyneema wire and the exerted force of a spring. The wing deployment is assured by resistors redundant assembly. When supplied, the blocking wire of Dyneema burns and consequently, mechanical spring system will deploy the wings. Current telemetries are available on each thermal cutter.

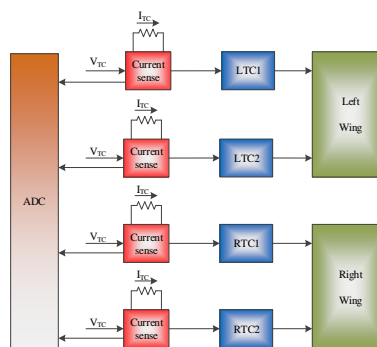


Figure 8 – Thermal cutters

### 3.3. Stepper motors

Two micro stepper motors handle the solar panels sun pointing. Between slip ring and wing assembly a gearhead is present to improve the motor torques. The motor motion is achieved by two H-bridge MOSFET configuration showed in Figure 9.



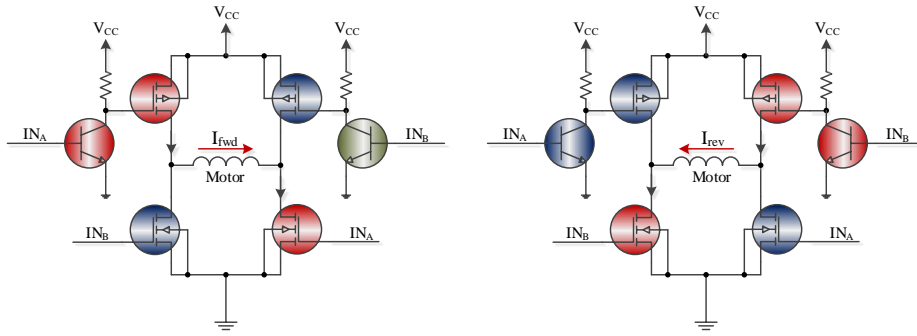


Figure 9 – H-bridge motor drive

When input A is active, a forward current will flow through the motor phase, while a reverse current will flow when input B is active. Due to the presence of gearhead, we can simplify the motor phase signal control using a full step signal pattern.

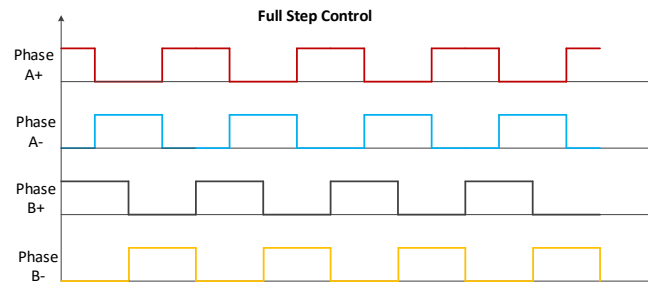


Figure 10 – Full step waveform signals

### 3.4. Sun sensors

The maximum power point tracking is achieved by means of two photodiodes with different sensitivity. The coarse sensor (on the left) is used for sun pointing when the solar panels are far from the maximum power point. Due to the better responsivity near the orthogonal light direction incidence, the fine sensor (on the right) is used to improve the sun tracking around the maximum power point.

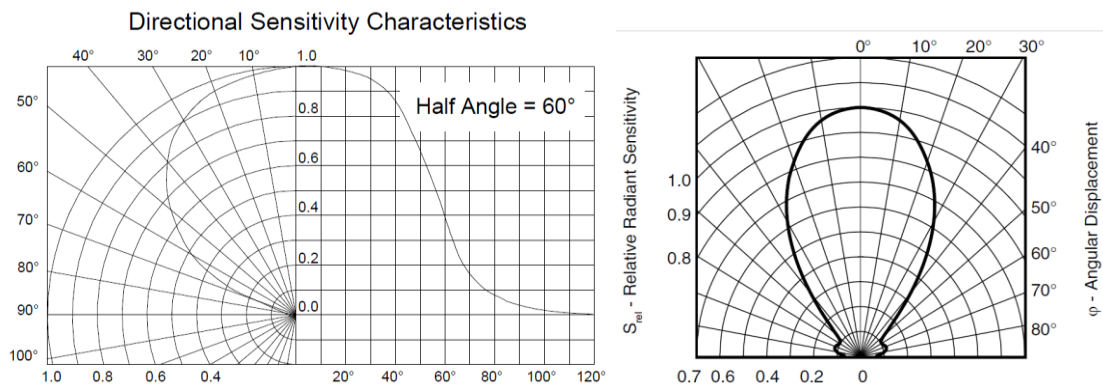


Figure 11 – Photodiodes sensitivity graphs

Low noise, high gain trans-impedance stages are used to amplify the low current signals coming from photodiodes. 2-poles Butterworth filters are used to cut out the high frequency noise.

### **3.5. Solar Array Control subsystem**

The SAC board is equipped with two independent motor control drives, the power handling stage for the thermal cutters and a microcontroller for the scheduling and telemetry acquisitions. It can communicate with the CubeSat OBDH through I<sup>2</sup>C or CAN BUS interfaces. The solar panel power is not handled by the SAC, but routed out to EPS subsystem through two Molex PicoBlade<sup>®</sup> connectors. All connections are redundant. The control law is written using C language code and is stored in the internal flash memory of the MCU. A watch-dog timer assures that the sun pointing algorithm will continue if firmware freeze.

## **4. CONTROL LAW**

The control law of the SAC, regulating the solar pointing, is based on a classical MPPT (Maximum Power Point Tracking) algorithm, in particular the idea of the Perturb and Observe (P&O) is used to accomplish the proposed task. Through a stage of trans-impedance, the voltage feedback from the two photodiodes, mounted on each wing of the SADA, is used to obtain a current feedback to align the Solar Arrays with the Sun direction.

### **4.1. Filter**

Before starting with the explanation of the algorithm, it is worth to say that the three main panels, composing a whole wing, are coupled by hinges and springs and during in orbit maneuvers there it might be the possibility of arise oscillations that must be filtered out. So, in order to get more reliable measures from the photodiodes, a filter from the software side has been introduced.

In order to minimize the CPU intervention, data from the peripherals are transferred into the RAM using the DMA mechanism. Since the DMA controller uses a dedicated bus for data transfers, it does not lose cycles from the code execution flow of the CPU. The idea is to use a sliding window in the acquisitions, in particular four measures are compared. The variance value is computed using Bessel's correction, in order not to have a biased estimation. In addition, the control is done based on the Mahalanobis distance to check if the oscillations are damped.

### **4.2. Control Algorithm**

Once the measures are stable, the control algorithm is executed. Since the rotary mechanism is independent for the left and the right side, also the control of the two wings is independent. Looking

at the evolution of the sensed currents, with the respect to the elevation angle (Figure 12), it can be seen that, during control, switching from one measure to another can lead to a more precise tracking. In particular, four areas can be identified.

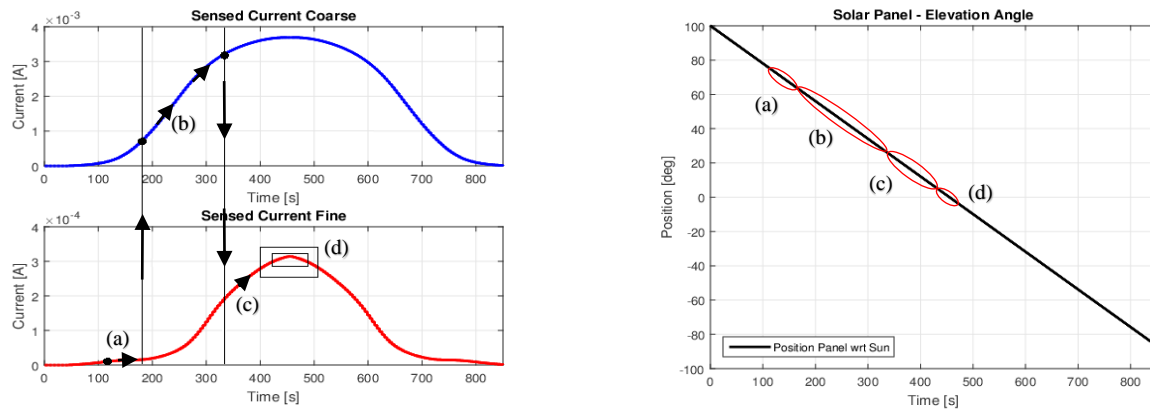


Figure 12 - Sensed Currents (left) for different Elevation Angles (right) and Zero Azimuth.

The evolutions of the photodiode currents in Figure 12 have been obtained through simulations in Matlab/Simulink® environment, where the SADA architecture, composed by the stepper motor, the driver, the gearhead and sun sensors have been implemented. In particular, the characteristics of responsivity of the photodiodes and in orbit conditions, such as the solar constant of  $1.367 \text{ kW}/\text{m}^2$  (AM0), have been used to get reliable results and recreate the SADA working conditions. Laboratory tests have confirmed the behavior of the current's curve. The results will be presented in chapter 5. For elevation angles in zone “b”, the maximum power point is still far and it is convenient to use the coarse sensor, since the slope remains almost constant and behaves better with the respect to the fine sensor. The best responsivity of the fine sensor can be used to make the solar panels sensitive to elevation angles at almost  $90^\circ$  and do solar tracking even at some critical angles. The working point will be, in this case, in the zone “a” of Figure 12. Executing the control action, based on the sign of the variation of current between two time intervals, will bring the panels to the zone “c”, where the slope of the coarse sensor is very tight, so a switch on the fine sensor is done in order to enhance tracking, since here we are almost on the maximum power point. At the end, in order to avoid chattering around the point of maximum, zone “d” is identified, where even the slope of the fine sensor is small.

During the following iterations, even if the sensed currents are changed, there is the possibility to check if moving is convenient, looking at Figure 12 means that, if we are still in the greater box in the zone “d”, no action is taken.

## 5. TESTS AND RESULTS

Hardware and functional tests were performed to confirm the reliability of the overall system. Furthermore, radiation tests were performed on the main analog and digital components like MCU, analog temperature sensor and anti-latchup system achieving good results up to 20Krad. Focused on the analog photodiode outputs, no variations were observed during irradiation test.

### 5.1. Functional Verification in Laboratory Environment

To verify the fundamental functional of SADA, the following tests have been done:

- Deployment test (life test in accordance to ECSS-E-ST-33-01C);
- Sensor calibrations;
- System calibration;
- Measure and Compensation of Backlash;
- Functional Verification of Tracking Algorithm.

During the functional tests, when was requested a rotation of solar panels, dummy arrays were used. The dummy array has the same inertia and mass of the real solar panel but, the stiffness, is different. The solar array doesn't have the sufficient stiffness to work at ground without complex off-loading system. Therefore, the dummy inertia can be used to facilitate the ground test operations.

### 5.2. Deployment test

In accordance to ECSS-E-ST33-01C, the lifetime qualification has to be verified using the factored sum of the predicted nominal ground test cycles and the in-orbit operation cycles. The expected ground test deployment cycles are 3 and in orbit is 1. Total of 22 cycles have been done to verify the duration of deployment mechanism and, after the test, all measured performances have been found compliant to the requirements. The Figure 13 shows a deployment phase.

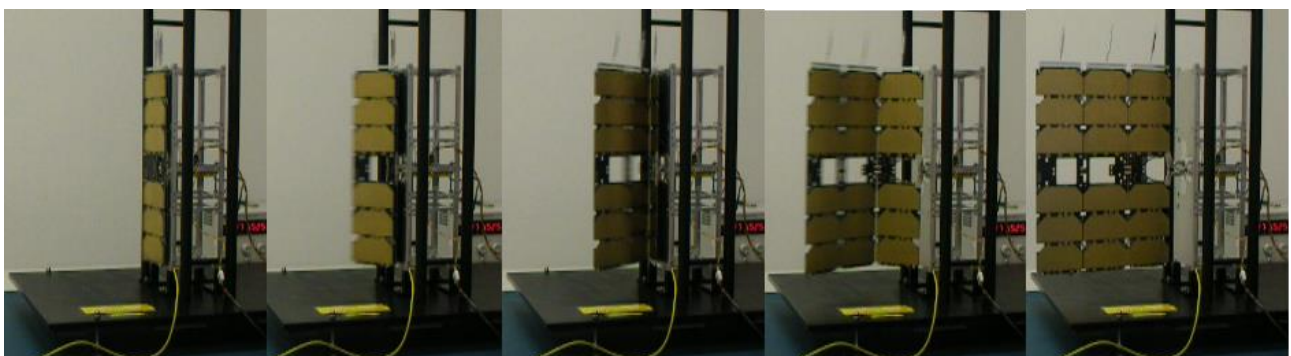


Figure 13 – Solar wing deployment sequence

### 5.3. Calibration Sensors

To increase the precision given by sun sensors, analog measures have been done for both wings. The analog values highlight that sensors have an offset of:

	<i>Left Wing</i>	<i>Right Wing</i>
<i>Coarse</i>	$2\ \mu\text{A}$	$1\ \mu\text{A}$
<i>Fine</i>	$20\ \text{nA}$	$0.5\ \mu\text{A}$

These values are taken into account in the control algorithm to increase the measures resolution. Figure 14 shows the comparison between the analog data acquired from the oscilloscope and the digital data filtered via firmware. What is worth to point out is that, thanks to the hardware filters, the analog measures are not too noisy and fit well the digital data.

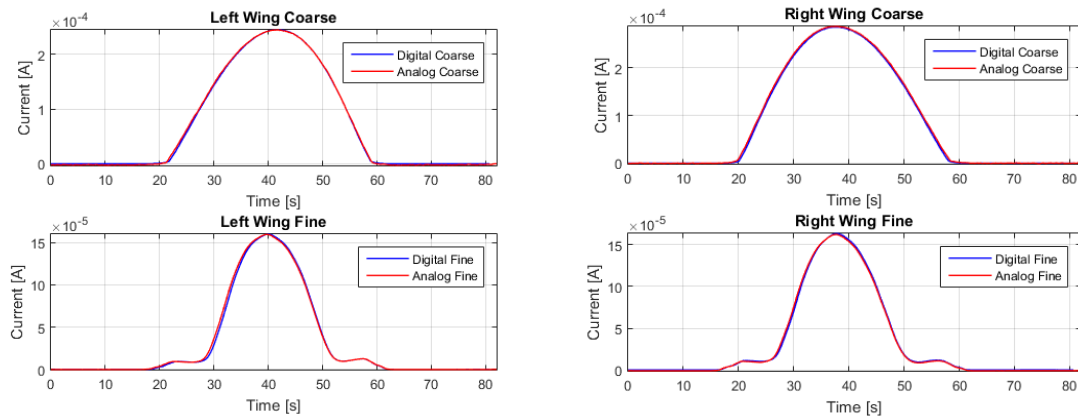


Figure 14 - Comparisons of analog and filtered data from the photodiodes

### 5.4. Calibration System

The aims of calibration system procedure are:

- Verify the repeatability of the measures;
- Verify the sensor response at different solar radiance.

The tests have been conducted in laboratory and lamps have been used as illuminance source. In the first test, the scope is to verify that slip rings, during several rotations, doesn't perturb the measures. In order to do that, 3 groups of 3 cycles have been implemented. Each cycle is composed by a 360° turn of the dummy panels.

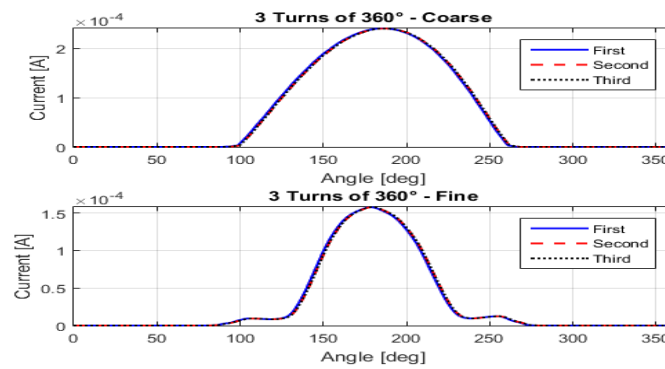


Figure 15 – Current measures from 3 turns of 360°

From Figure 15 can be seen that repeatability of the measures has been verified. The maximum offset of each curve to the others is about 0.2%. This value is compatible to the requirement of 5° pointing accuracy of the SADA.

Furthermore, as verified in the second test, the curves are aligned during illuminance variations (Figure 16, left). The system works well and in the same way in different conditions, corresponding to different Sun directions (azimuth and elevation). The repeatability of the measures has been tested even during illuminance variations (Figure 16, right).

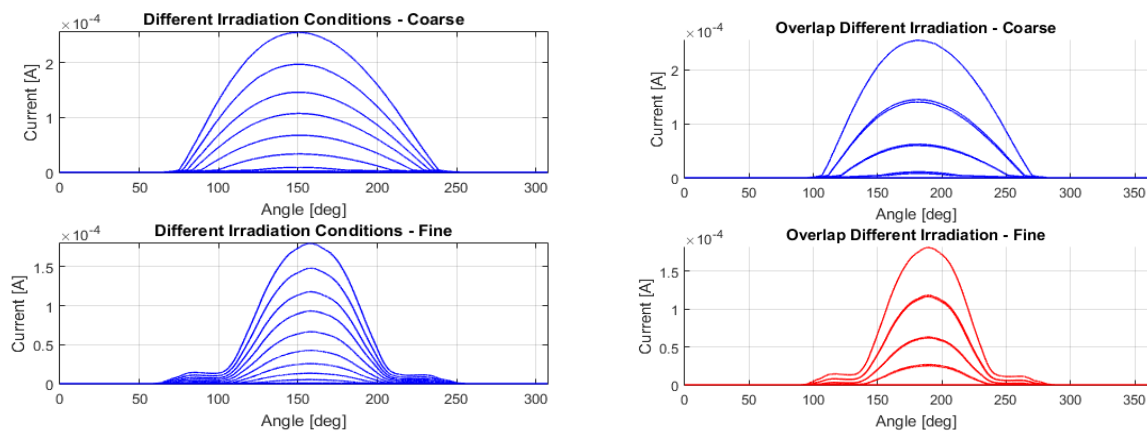


Figure 16 – Curves of current during different irradiance conditions

### 5.5. Measure and Compensation of Backlash

To increase the pointing accuracy, functional tests for studying the backlash of the SADA have been done. Groups of tests of 2 cycles have been executed. On each test, after a complete turn of 360° counterclockwise (CCW), the motion has been inverted and 360° clockwise (CW) have been done. All the results showed that the measured backlash of the whole system is of 3.8° for both wings.

Backlash has been compensated via firmware. Validation tests have been done and the Figure 17 shows the results before the backlash compensation (left), which exhibit a maximum displacement between the curves of about  $20\mu\text{A}$  (Fine Sensor) and after (right), with a maximum displacement of about  $2\mu\text{A}$  (Fine Sensor). The backlash compensation has been validated also making long run simulations, where cycles of 5 inversions have been executed.

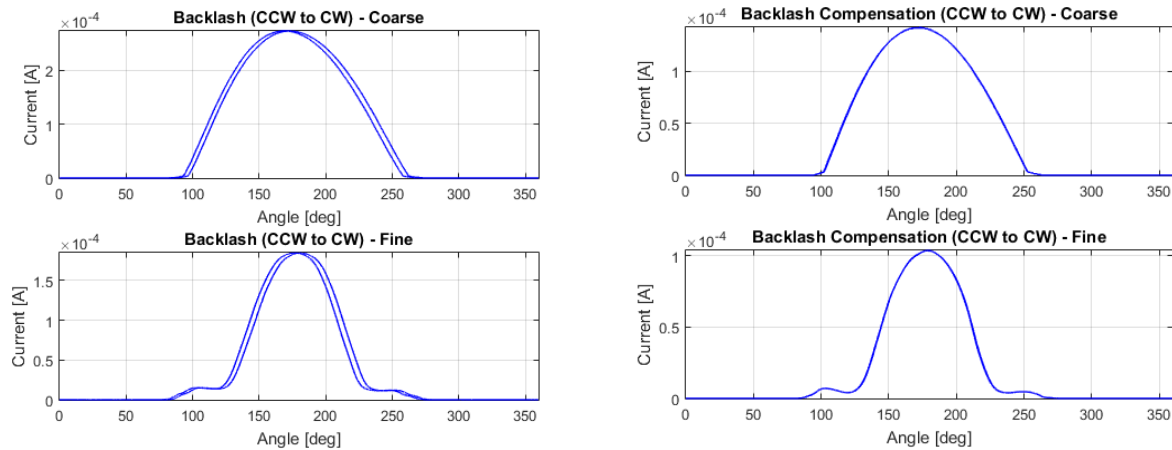
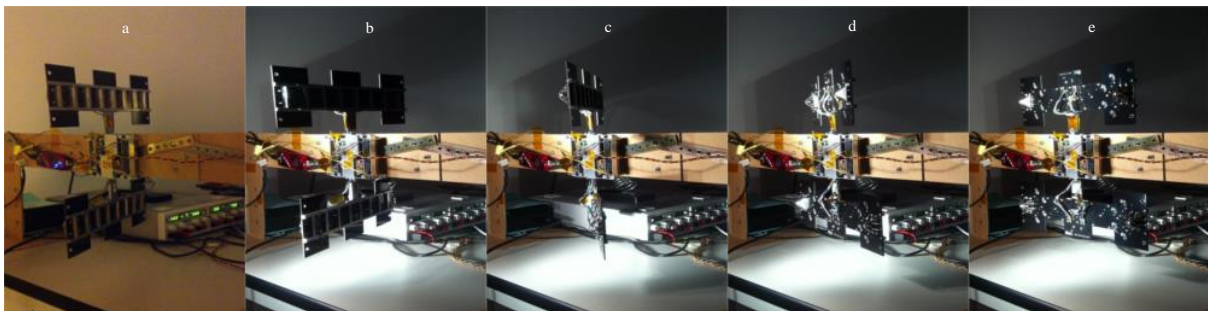


Figure 17 – Sensed currents during inversion; with backlash (left) and with compensation (right)

## 5.6.Functional Verification of Tracking Algorithm

Moreover, functional verifications have been accomplished in order to validate the performance of the tracking algorithm. After a  $360^\circ$  turn, during which the value of the maximum current has been computed, the tracking algorithm has been executed. The behavior of the sensed current during tracking can be seen in Figure 18. The tests exhibit a pointing accuracy  $< 5^\circ$ .





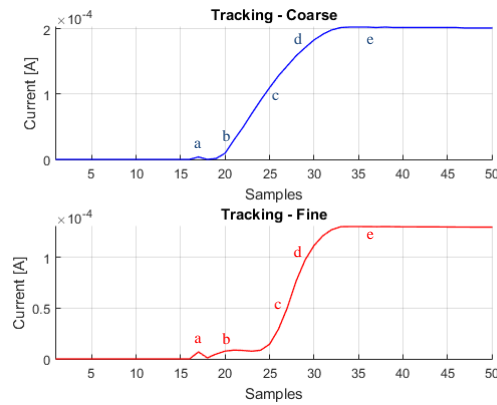


Figure 18 – Evolution of the currents during tracking

## 5 CONCLUSIONS

Preliminary functional tests, confirm the following specifications:

<b>Power Transfer Output:</b>	<i>max. 43W (3A @ channel)</i>
<b>Output Torque:</b>	<i>25 mNm</i>
<b>Pointing accuracy:</b>	<i>&lt; 5°</i>
<b>Step size:</b>	<i>0.004°</i>
<b>Configuration:</b>	<i>2 Solar Arrays (2 Channels)</i>
<b>Release Mechanism:</b>	<i>2 x 1.7A for each Solar Array</i>
<b>Range of Motion:</b>	<i>Free rotation thanks to the Slip Rings</i>
<b>Sensors:</b>	<i>2 sun detection, fine and coarse for each Solar Array, temperature</i>
<b>Power Consumption:</b>	
<b>Idle:</b>	<i>160mA</i>
<b>Holding:</b>	<i>430mA</i>
<b>Tracking:</b>	<i>450mA</i>
<b>Mass:</b>	
<b>SAC:</b>	<i>185 gr</i>
<b>WING:</b>	<i>275 gr (331 gr with wall panel and Thermal cutter) without solar cells</i>
<b>Total:</b>	<i>850 gr</i>
<b>Compliant to:</b>	<i>Cubesat Standard.</i>
	<i>Baseline: 3U structure</i>

## 6 REFERENCES

- [1] POR FESR LAZIO 2007/2013 – REGIONE LAZIO – Asse I – Attività 2 - Microinnovazione.
- [2] Small Spacecraft Technology State of Art NASA/TP-2014-216648/REV1.